Antibacterial and physical properties of calcium-phosphate and calcium-fluoride nanocomposites with chlorhexidine

Lei Cheng[1,2], Michael D. Weir[1], Hockin H. K. Xu[1,3-5], Alison M. Kraigsley[6], Nancy Lin[6], Sheng Lin-Gibson[6], Xuedong Zhou[2]

[1]Biomaterials & Tissue Engineering Division
Dept. of Endodontics, Prosthodontics and Operative Dentistry
University of Maryland Dental School, Baltimore, MD 21201, USA
[2]State Key Laboratory of Oral Diseases, West China College of Stomatology
Sichuan University, Chengdu, China
[3]Center for Stem Cell Biology & Regenerative Medicine
[4]University of Maryland Marlene and Stewart Greenebaum Cancer Center
University of Maryland School of Medicine, Baltimore, MD 21201, USA
[5]Department of Mechanical Engineering, University of Maryland, Baltimore County, MD 21250
[6]National Institute of Standards & Technology, Gaithersburg, MD 20899, USA

Correspondence:
Dr. Hockin H. K. Xu, Professor, Director of Biomaterials & Tissue Engineering Division, Department of Endodontics, Prosthodontics and Operative Dentistry, University of Maryland Dental School, Baltimore, MD 21201 (Email: hxu@umaryland.edu), and Dr. Xuedong Zhou, Professor, Dean, West China College of Stomatology, Sichuan University, China (Email: zhouxd@scu.edu.cn).

Short title: Antimicrobial calcium phosphate and fluoride nanocomposites with chlorhexidine

Key words: dental nanocomposite, calcium phosphate, calcium fluoride, chlorhexidine, stress-bearing, *S. mutans* biofilm, caries inhibition.

Abstract

Secondary caries limits the longevity of tooth restorations. The replacement of existing restorations accounts for 50-70% of all restorations. Replacement dentistry costs $5 billion in the U.S. annually. The objectives of this study were to (1) develop nanocomposites containing amorphous calcium phosphate (ACP) nanoparticles, calcium fluoride (CaF_2) nanoparticles, and chlorhexidine (CHX), and (2) investigate the effects of these nanocomposites on *Streptococcus mutans* (*S. mutans*) biofilm formation and lactic acid production for the first time. Four nanocomposites were fabricated with fillers of: Nano ACP; nano ACP + 10% CHX; nano CaF_2; nano CaF_2 + 10% CHX. A commercial composite with fluoride release, a composite without fluoride release, and a resin-modified glass ionomer were also tested. Compared to commercial composites, ACP nanocomposite had minimal antibacterial property, and CaF_2 nanocomposite was moderately antimicrobial. Adding CHX to ACP and CaF_2 nanocomposites rendered them strongly antimicrobial. ACP and CaF_2 nanocomposites containing CHX maintained a *S. mutans* media pH of above 6.5, while the pH for commercial composites decreased to 4.2. Nanocomposites with CHX reduced the biofilm acid production and metabolic activity by 10-20 folds, compared to a commercial composite. Colony-forming units of nanocomposites with CHX were orders of magnitude less than that of a commercial composite. Mechanical properties of nanocomposites with CHX were similar to a commercial composite without fluoride nor CHX. In conclusion, the novel nanocomposites could not only release calcium phosphate ions to remineralize the existing lesions, release fluoride to form fluoroapatite to resist acid attacks, but also inhibit biofilm formation and lactic acid production. These antimicrobial, remineralizing, and mechanically-strong nanocomposites may be promising for tooth cavity restorations with anti-caries capabilities.

1. Introduction

Nearly 200 million dental restorations are placed annually in the U. S. [1]. Resin composites are increasingly popular for tooth cavity restorations because of their esthetics and direct-filling capability [2-8]. Remarkable progresses have led to esthetic composite restoratives with less removal of tooth structures, enhanced load-bearing properties, and improved clinical performance [9-15]. However, secondary caries at the restoration margins is identified as a main limitation to the longevity of the restorations [16-18]. The replacement of existing restorations accounts for 50-70% of all restorations [19,20]. Replacement dentistry costs $5 billion annually in the U. S. alone [21]. Tooth caries is a dietary carbohydrate-modified bacterial infectious disease, and is one of the most common bacterial infections in humans [22-24]. The basic mechanism of caries is demineralization through the attack by acid generated by bacteria [25-27]. Hence, acidogenic bacteria growth and biofilm formation with exposure to fermentable carbohydrates are responsible for caries. However, resin composites did not hinder bacteria colonization and plaque formation. On the contrary, studies showed that composites allowed more accumulation of plaque on their surfaces than other restoratives [28-30].

Efforts are underway to develop novel antibacterial composites to inhibit caries. One approach involved antibacterial monomers which inhibited the growth and plaque accumulation by bacteria such as *Streptococcus mutans* (*S. mutans*) [4,29,31]. A polymerizable bactericidal monomer, 12-methacryloyloxydodecylpyridinium bromide (MDPB), was immobilized in the resin which reduced bacteria growth via contact inhibition [4]. In another approach, ionic liquid dimethacrylate monomers that contained quaternary ammoniums groups were used to develop antimicrobial resins, which reduced bacterial colonization [32]. Other studies employed chlorhexidine (CHX), a strong bactericide against caries-associated bacteria, which resulted in

CHX release and reduced bacteria growth [33-35]. CHX was also incorporated into glass ionomer cements [36], and a great increase in the inhibition zone was obtained [37].

Another promising class of composites consisted of calcium phosphate (CaP) particles of about 1 μm to 55 μm in sizes [38-40]. They released supersaturating levels of calcium (Ca) and phosphate (PO_4) ions and remineralized tooth lesions *in vitro* [39,40]. In recent studies, CaP nanoparticles of about 100 nm in size were synthesized via a spray-drying technique for the first time [41,42]. Composites containing CaP nanoparticles with high surface areas released high levels of Ca and PO_4 while possessing mechanical properties nearly two-fold those of previous CaP composites [41,42]. Nanocomposites containing CaF_2 nanoparticles were also developed that released fluoride (F) ions matching that of a resin-modified glass ionomer [43,44]. The mechanical properties of the CaF_2 nanocomposite were much higher than that of resin-modified glass ionomer, and matched those of commercial composites with little F release. However, there has been no report on CaP and CaF_2 nanocomposites containing CHX to achieve the triple benefits of remineralization, antibacterial, and load-bearing capabilities.

Therefore, the objectives of this study were to combine CHX with CaP and CaF_2 nanoparticles into the nanocomposites, and to determine mechanical and antibacterial properties. It was hypothesized that: (1) Incorporating CHX will impart a potent bactericidal capability to the CaP and CaF_2 nanocomposites to diminish the *S. mutans* colony forming units and lactic acid production; and (2) the mechanical properties of the CaP and CaF_2 nanocomposites containing CHX will match those of commercial composite with no ion release nor antibacterial capability.

2. Materials and methods

2.1 Fabrication of CaP and CaF_2 nanocomposites containing CHX

Nanoparticles of amorphous calcium phosphate (ACP), $Ca_3(PO_4)_2$, were synthesized via a spray-drying technique in a recent study for the first time [45]. ACP is an important compound because it is a precursor that can convert to apatite, similar to the minerals in tooth enamel and dentin. Briefly, a spraying solution was prepared by dissolving calcium carbonate ($CaCO_3$, Fisher, Fair Lawn, NJ) and dicalcium phosphate anhydrous ($CaHPO_4$) (J. T. Baker, Phillipsburg, NJ) into an acetic acid solution. It had Ca and PO_4 ionic concentrations of 8 mmol/L and 5.333 mmol/L, respectively [45]. This yielded a Ca/P molar ratio of 1.5, the same as that for ACP. This solution was sprayed through a nozzle that was situated on a spray chamber [46]. The water and volatile acid were evaporated into the heated column and expelled from an electrostatic precipitator into an exhaust-hood. The dried particles were collected by the electrostatic precipitator [45]. A multipoint-BET (Brunauer, Emmet, and Teller) method measured a specific surface area of 17.76 m^2/g for collected powder, yielding an ACP particle size of 116 nm, which was consistent with transmission electron microscopy examinations [45].

CaF_2 nanoparticles were synthesized using the same spray-drying apparatus, except that a two-liquid nozzle was employed [43,47]. This allowed two solutions to be mixed during atomization: a calcium solution, $Ca(OH)_2$, and a fluoride solution, NH_4F. The two solutions were atomized into the heated chamber, leading to the formation of CaF_2 nanoparticles: $Ca(OH)_2 + NH_4F \rightarrow CaF_2 + NH_4OH$. The NH_4OH was removed as NH_3 and H_2O vapors [47]. The BET method measured a surface area of 35.5 m^2/g, yielding a CaF_2 particle size of 53 nm [43].

Chlorhexidine diacetate (Sigma, St. Louis, MO) was frozen via liquid nitrogen, and then ground in a mortar and pestle to obtain a fine particle size. The particles were sputter coated

with gold and examined in a scanning electron microscope (SEM, FEI Quanta 200, Hillsboro, OR). The particles are referred to as CHX and incorporated into dental resins.

Barium boroaluminosilicate glass particles with a median diameter of 1.4 μm (Caulk/Dentsply, Milford, DE) were used as a co-filler to reinforce the nano ACP and CaF_2 composites [44,45]. The glass particles were silanized with 4% (all mass fractions) 3-methacryloxypropyltrimethoxysilane and 2% n-propylamine. For ACP nanocomposite, a resin of Bis-GMA (bisphenol glycidyl dimethacrylate) and TEGDMA (triethylene glycol dimethacrylate) at 1:1 mass ratio was rendered light-curable with 0.2% camphorquinone and 0.8% ethyl 4-N,N-dimethylaminobenzoate [45]. For the CaF_2 nanocomposite, a two-part chemically-activated resin was used due to the relative opacity of the paste. The initiator resin consisted of 48.975% Bis-GMA, 48.975% TEGDMA, 0.05% 2,6-di-*tert*-butyl-4-methylphenol, and 2% benzoyl-peroxide. The accelerator resin consisted of 49.5% Bis-GMA, 49.5% TEGDMA, and 1.0% *N*,*N*-dihydroxyethyl-*p*-toluidine [44].

Four nanocomposites were made with the following fillers: (1) 30% nano ACP + 35% glass (referred to as "Nano ACP"); (2) 30% nano ACP + 25% glass + 10% CHX (referred to as "Nano ACP + CHX"); (3) 30% nano CaF_2 + 35% glass ("nano CaF_2"); (4) 30% nano CaF_2 + 25% glass + 10% CHX ("nano CaF_2 + CHX").

The glass and nanoparticle filler levels were selected following previous studies [44,48]. The CHX filler level was based on previous studies which ranged from 0.5% to 33% [33-36]. The total filler mass fraction of 65% yielded a readily mixed cohesive paste. The paste was placed into longitudinal molds of 2 x 2 x 25 mm for mechanical testing, and disk molds of 12 mm in diameter and 2 mm in thickness for bacteria experiments. The nano ACP composite specimens were photo-cured (Triad 2000, Dentsply, York, PA) for 1 min on each side. CaF_2

composite specimens were self cured. The specimens were then incubated at 37 ℃ for 24 h.

Three commercial materials were tested as comparative controls. A resin-modified glass ionomer (Vitremer, 3M, St. Paul, MN) is referred to as "RMGI". It consisted of fluoroaluminosilicate glass, and a light-sensitive, aqueous polyalkenoic acid. Indications include Class III, V and root-caries restoration, Class I and II in primary teeth, and core-buildup. A powder/liquid mass ratio of 2.5/1 was used according to the manufacturer. A composite with nanofillers of 40 nm to 200 nm and a low level of F release was used (Heliomolar, Ivoclar, Ontario, Canada) (referred to as "CompositeF"). The fillers were silica and ytterbium-trifluoride with a filler level of 66.7%. Heliomolar is indicated for Class I and Class II restorations in the posterior region, Class III and Class IV anterior restorations, Class V restorations, and pit and fissure sealing. Renamel (Cosmedent, Chicago, IL) served as a non-releasing control, and is designated as "CompositeNoF". It consisted of nanofillers of 20 nm to 40 nm with 60 % fillers in a multifunctional methacrylate ester resin [49]. Renamel is indicated for Class III, IV, and V restorations. Specimens were photo-cured in the same manner as the ACP nanocomposite.

2.2 Flexural testing

Flexural strength and elastic modulus were measured using a three-point flexural test with a 10 mm span at a crosshead-speed of 1 mm/min on a computer-controlled Universal Testing Machine (5500R, MTS, Cary, NC). Flexural strength was calculated by: $S = 3P_{max}L/(2bh^2)$, where P_{max} is the fracture load, L is span, b is specimen width and h is thickness. Elastic modulus was calculated by: $E = (P/d)(L^3/[4bh^3])$, where load P divided by displacement d is the slope of the load-displacement curve in the linear elastic region. Specimens were immersed in water at 37 ºC for 1 day (d) and 28 d prior to mechanical testing.

2.3 Chlorhexidine (CHX) release measurement

CHX release was measured for the nano ACP + CHX composite and the nano CaF_2 + CHX composite. A physiological-like buffer solution (133 mM NaCl, 50 mM 4-(2-hydroxyethyl)-1-piperazineethanesulfonic acid, HEPES) with pH of 7 was prepared. Following previous studies [41-44], three specimens of approximately 2 x 2 x 12 mm were immersed in 50 mL of the solution. The concentrations of CHX released from the specimens were measured at 1, 2, 3, 7, 14, 21, and 28 d. At each time period, aliquots of 200 μL were removed and replaced by fresh solution. A series of chlorhexidine reference solutions was prepared and a standard curve was constructed. The absorbance at 255 nm was measured by using a microplate reader (SpectraMax M5, Molecular Devices, Sunnyvale, CA) and the CHX quantity was calculated using the known standard calibration curve.

2.4 *S. mutans* inoculation and pH measurement

The use of *S. mutans* bacteria (ATCC 700610, American Type Culture**,** Manassas, VA**)** was approved by the University of Maryland. *S. mutans* is a cariogenic, aerotolerant anaerobic bacterium, identified as the primary causative agent of dental caries [22]. Fifteen μL of stock bacteria was added into 15 mL of a growth media consisting of brain heart infusion (BHI) broth (BD, Franklin Lakes, NJ) supplemented with 0.2% sucrose in a tube, which was cultured at 37 ºC with 5% CO_2 in an incubator for 16 h. During this culture, the *S. mutans* were suspended in the BHI broth in planktonic form. After 16 h, this media with *S. mutans* was diluted by 10-fold to form the inoculation media [50]. The BHI broth with 0.2% sucrose, but without the bacteria, is termed the "growth media".

Each composite disk was placed in a well of a 24-well plate, then 1.5 mL of the

inoculation media was added to each well. The samples were incubated anaerobically in an incubator with 5% CO_2 and 37 ºC for 24 h, which formed the initial biofilm on the disk. At 24 h, each disk with biofilm on it was transferred to a new 24-well plate containing 1.5 mL of fresh growth media. The pH of the media was measured via a pH meter (Accumet Excel XL25, Fisher, Pittsburgh, PA) from 24 h to 48 h. This pH was solely related to the biofilm on the composite, because there was no interference of planktonic bacteria in the media. At 28 h, each disk with biofilm on it was transferred to a new 24-well plate containing 1.5 mL of fresh growth media. The pH of the media was measured from 48 h to 72 h.

2.5 Live/dead bacteria staining

Each composite disk in a well of a 24-well plate was inoculated with 1.5 mL of the inoculation media, and cultured for 1 d (initial biofilm), or 3 d (mature biofilm). For the 3 d culture, the growth media was changed once a day, by preparing a new 24-well plate filled with fresh growth media, and then transferring the composite disks to the new plate. After 1 d or 3 d, the biofilms on the disks were stained using a live/dead bacterial viability kit (Molecular Probes, Eugene, OR). Live bacteria were stained a green fluorescence, and dead bacteria were stained a red fluorescence. The stained disks were imaged using a laser scanning confocal microscopy (LSM 510, Zeiss, Germany). Five images were collected at random locations on each disk. Three disks were evaluated for each material at each time period.

2.6 Lactic acid production and CFU counts

After 3 d culture, mature biofilm was formed on the composite disk. Each disk with biofilm on it was rinsed in cysteine peptone water (CPW) to remove loose bacteria, and was

placed in a 24-well plate. Then, 1.5 mL of buffered peptone water (BPW) supplemented with 0.2% sucrose was added to each well. The reason for using the BPW media was that the mature biofilm would not grow and would remain stable when cultured in this media for 3 h, while producing acid. In addition, BPW has a relatively high buffer capacity hence the pH would not become significantly acidic, as a low pH could hinder bacterial acid production. The samples were incubated anaerobically in an incubator with 5% CO_2 and 37 ºC for 3 h to allow acid production by the biofilms. After 3 h, the BPW solutions were stored for lactate analysis.

At this stage, the disks with the mature biofilms were transferred into tubes with 2 mL CPW, and the biofilms were harvested by sonication and vortexing at the maximum speed for 20 seconds using a vortex mixer (Fisher, Pittsburgh, PA). This separated the biofilm into individual bacteria, and the bacterial suspension was serially diluted in CPW and plated on BHI agar plates. After 3 d, a single bacterium grew and became a colony, showing as a group of bacteria on the agar plate which resulted from a single bacterium on the composite disk. After incubating the agar plate anaerobically in an incubator with 5% CO_2 and 37 ºC for 3 d, the number of colonies was counted on the agar plate. This data, coupled with the folds of dilution, led to the calculation of the total colony-forming units (CFU) from an entire composite disk.

Lactate concentrations in the BPW solutions were determined by using a microplate reader (SpectraMax M5, Molecular Devices, Sunnyvale, CA). Standard curves were made by using a standard lactic acid (Supelco Analytical, Bellefonte, PA). An enzymatic (lactate dehydrogenase) method was used to measure the absorbance at 340 nm (optical density OD_{340}) for the collected BPW solutions via the microplate reader [51].

2.7 MTT assay

Each composite disk in a well of a 24-well plate was inoculated with 1.5 mL of the inoculation media, and cultured for 1 d or 3 d. Each disk with the biofilm was then transferred to a new 24-well plate for MTT assay, which is a colormetric assay that measures the enzymatic reduction of MTT to formazan [52]. MTT refers to 3-(4,5-Dimethylthiazol-2-yl)-2,5-diphenyltetrazolium bromide, a yellow tetrazole. One mL of MTT dye (5 mg/mL MTT in PBS) was added to each well and incubated at 37 ℃ in 5% CO_2 for 1 h. During this process, the bacteria metabolized the MTT and reduced it to purple formazan inside the living cells. After 1 h, the disks with biofilms were transferred to a new 24-well plate, 1 mL of dimethyl sulfoxide (DMSO) was added, and the plate was incubated for 20 min with gentle mixing at room temperature. DMSO could dissolve the purple formazan into a colored solution [52]. After brief mixing via pipetting, 200 μL of the DMSO solution from each well was transferred to a 96-well plate, and the absorbance OD_{540} was measured via the microplate reader. A higher absorbance indicates a higher formazan concentration, which in turn indicates a higher number of live bacteria on the composite disk that metabolized the MTT.

One-way and two-way ANOVA were performed to detect the significant effects of the variables. Tukey's multiple comparison test was used to compare the data at a p value of 0.05.

3. Results

Fig. 1 shows SEM micrographs of the ground CHX, with a pile of particles at a lower magnification in (A), and dispersed particles at a higher magnification in (B). The histogram of CHX particle size distribution is plotted in (C). The particle size ranged from approximately 0.1 μm to 5 μm, with (mean ± sd; n = 100) of (0.62 ± 0.48) μm. The CHX release from the ACP nanocomposite and CaF_2 nanocomposite is plotted in (D) (mean ± sd; n = 3). The CHX release

from the ACP nanocomposite was similar to that of the CaF_2 nanocomposite ($p > 0.1$).

Mechanical properties are plotted in Fig. 2: (A) Flexural strength, and (B) elastic modulus, after 1 d and 28 d of immersion. CompositeF, nano ACP composite, nano CaF_2 composite, and nano CaF_2 + CHX composite had a significant decrease in strength from 1 d to 28 d ($p < 0.05$). CompositeF, CompositeNoF, nano ACP, and nano CaF_2 had strengths similar to each other at 28 d ($p > 0.1$). The strengths of nano ACP + CHX and nano CaF_2 + CHX at 28 d were about 2-fold that of RMGI ($p < 0.05$). Elastic moduli in general were similar to each other for the different materials at 1 d and 28 d.

The pH of the biofilm media is plotted in Fig. 3. (A) The pH measurement was started at 24 h, when the media was changed. (B) Then the pH was measured again after the media change at 48 h. In (A), for nano CaF_2 + CHX and nano ACP + CHX composites, the pH stayed at 6.5 or higher. For all other materials, the pH decreased with time, reaching 4.7 for RMGI, 4.6 for nano CaF_2 composite, and 4.2 for the other composites at 48 h. Comparing (A) with (B) shows a similar trend and similar end pH values, indicating that the effect of inhibiting bacteria growth and acid production for the CHX composites was maintained in 3 d.

Live/dead staining photos are shown in Fig. 4. At 1 d, the bacteria were predominantly alive in (A) to (C); CompositeNoF and CaF_2 nanocomposite had similar features. However, in (D), nano ACP + CHX composite had mostly dead bacteria, similar to that of nano CaF_2 + CHX composite. At 3 d, the *S. mutans* had formed a mature and dense biofilm in (E) to (G), where the bacteria were primarily alive. CompositeNoF and CaF_2 nanocomposite had qualitatively similar features as those in (E) to (G). In contrast, nano ACP + CHX composite in (H) had few bacteria on its surface, likely because the largely dead bacteria as shown in (D) were lost during media change. Nano CaF_2 + CHX composite yielded similar photos as (H).

Quantification of bacteria response is plotted in Fig. 5 for (A) lactic acid production, and (B) CFU counts. Biofilm on CompositeNoF produced the most acid, closely followed by that of nano ACP. Between F-releasing materials, biofilm on CompositeF had the most acid, while biofilms on nano CaF_2 composite and RMGI had similarly lower acid production. Acid production on composites with CHX was nearly 10-fold less than that on CompositeNoF. In (B), the CFU count was above 10^9 per disk for CompositeNoF, and slightly above 10^8 for all other materials without CHX. CFU counts for nanocomposites with CHX was reduced by 1,000-fold from that of CompositeNoF.

The MTT results are plotted in Fig. 6 for (A) 1 d, and (B) 3 d. In each plot, values (mean ± sd; n = 6) with dissimilar letters are significantly different ($p < 0.05$). In (A), CompositeNoF had the highest absorbance. The two nanocomposites containing CHX had absorbance 10-fold less than that of RMGI, and 20-fold less than that of CompositeNoF. A similar trend was maintained at 3 d in (B), although the absorbance was 1.5-2 fold higher than that at 1 d.

4. Discussion

The present study investigated the effects of novel nanocomposites containing ACP and CaF_2 nanoparticles and CHX on biofilm formation, bacteria CFU and acid production for the first time. An important approach to the inhibition of demineralization and the promotion of remineralization was the development of CaP composites [38-41]. Previous studies showed that the remineralization of tooth lesions was greatly promoted by increasing the solution calcium and phosphate ion concentrations [39,40]. Composites containing traditional CaP particles released Ca and PO_4 ions to supersaturating levels with respect to tooth mineral, and was shown to protect the teeth from demineralization, or even regenerate lost tooth mineral *in vitro* [39,40].

A recent study showed that the new nano ACP composite released Ca and PO_4 ions matching those of traditional CaP composites known to remineralize tooth lesions, while having much higher mechanical properties [45]. Another study demonstrated that the new nano CaF_2 composite released F ions at similar amounts to a commercial resin-modified glass ionomer, while having mechanical properties equivalent to a commercial composite without F release [44]. However, the incorporation of CHX into CaP composites was not reported.

CHX has been frequently used in dentistry such as in mouthrinses and is known to be a strong antimicrobial agent. The antimicrobial mechanism of CHX is not fully understood, and appears to be related to the destruction of cell walls by binding to glucan moieties [53], as well as the inhibition of cell replication [54]. CHX was incorporated into glass ionomer and resin-modified glass ionomer materials [36,37] as well as polymeric composites [33,35]. The present study showed that the CHX release was relatively high in the first week and then plateaued after 2 weeks (Fig. 1), which is similar to previous studies [36]. The percentage of CHX released from the ACP and CaF_2 nanocomposites after 28 d was about 2%, which is also comparable with previous studies. For example, the CHX released from a glass ionomer cement was about 3% to 5% after 240 d [36]. Another study showed that the percentage of CHX released from a resin composite was about 10% after 4 months of immersion in a pH 6 solution; when the solution pH was reduced to 4, the CHX release increased to 50% in 4 months due to polymer degradation [35]. The present study showed that even 2% of the CHX release from the nanocomposites greatly reduced bacteria CFU counts, biofilm formation, and lactic acid production. The 2% release indicates a large reservoir of CHX remaining in the composite. The present study used a model resin with Bis-GMA and TEGDMA at a 1:1 ratio, which is hydrophobic. The addition of water-absorbing monomer into the composite could improve diffusion and enhance CHX release.

It was estimated that if the CHX reservoir in the resin was fully utilized, the release could last 6 to 10 years [35]. Therefore, further study should incorporate a hydrophilic component such as 2-hydroxyethyl methacrylate (HEMA) and methacryloyloxyethyl phthalate (MEP) [40] to increase the CHX release, and to develop nanocomposites with controlled CHX release.

Most previous studies [33,34,36,37] did not mention attempts to obtain fine CHX particles by grinding the as-received particles, which was approximately 40 μm for the CHX diacetate from Sigma. A particle size of 40 μm is much larger than the glass fillers in dental composites, which are typically about 1 μm or less. One study reported the grinding of the as-received CHX, yielding a finer particle size of 13.5 μm [35]. Preliminary studies failed to obtain even smaller CHX particles, until the use of liquid nitrogen to chill the CHX powder followed by grinding. This appeared to embrittle and help shatter the particles, yielding an average size of 0.62 μm in the present study. A small CHX particle size is desirable because this could improve the polishability and mechanical properties of the composite. Previous studies on CHX incorporation into polymeric composites did not report their mechanical properties [33,35]. In the present study, the mechanical properties of the nanocomposites containing 10% CHX were measured after 1 d and 28 d immersion. Adding CHX decreased the strength of nano ACP and nano CaF_2 composites. At 28 d, the strength for nano ACP + CHX composite was approximately 80% that without CHX. A similar 20% strength loss occurred for the nano CaF_2 composite. However, the strength of the nanocomposites containing CHX was only slightly lower than the commercial composite control without CHX. The strength of the nanocomposites containing CHX was twice that of a resin-modified glass ionomer control.

Previous studies showed that bacteria colonize on surfaces to grow into a biofilm, which is a heterogeneous structure consisting of cell clusters embedded in an extracellular matrix [55].

Acidogenic bacteria such as *S. mutans* in the plaque metabolize carbohydrates to acids. Acid production causes demineralization to the tooth structure beneath the biofilm. This could result in the local plaque pH to drop to 4.5 or 4 after a sucrose rinse. Studies showed that there was a critical pH of about 5.5, below which demineralization dominates, leading to a net enamel mineral dissolution [56]. Therefore, it would be highly desirable for the restoration to maintain a local pH of above 5.5 in order to inhibit secondary caries at the restoration-tooth interface. Both the nano ACP + CHX composite and nano CaF_2 + CHX composite maintained a pH of 6.5 or higher, while the two commercial composites had pH below 4.5. Hence the nano ACP + CHX composite and the nano CaF_2 + CHX composite have the potential to maintain the local pH at a safe level to inhibit tooth mineral dissolution.

Another potential benefit of the nanocomposites to maintain a close-to-neutral pH at the biofilms is to modify the microenvironment of the plaque. This is because organic acids in the plaque can result in an increase in the proportion of acidogenic bacteria which have a high tolerance to acids (aciduric), at the expense of the other benign bacteria that are less acid-tolerant [22,57]. The normal plaque contains less than 1% of acidogenic bacteria in the oral flora [25]. However, repeated acidification in the plaque with an increasingly more acidic milieu results in the predominance of acidogenic and aciduric bacteria such as *S. mutans* [23]. Therefore, comparing with the commercial composites having a pH of 4.2 in the biofilm media, the new nanocomposites were able to maintain a pH of above 6.5, which may sustain the survival of benign bacteria and maintain a normal oral flora. This may help prevent the dominance of cariogenic bacteria and inhibit dental caries.

It is interesting to note that the nano CaF_2 + CHX composite had a higher pH than that of nano ACP + CHX composite. The mechanism for this is likely that the F ion release helped

reduce the acid production of the bacteria, via the inhibition of metabolic pathways such as the fermentation pathway for lactic acid production [55]. A previous study used a constant depth film fermentor (CDFF) model and showed that while F treatment had little effect on *S. mutans* viability, it did reduce the acid production of the bacteria [58]. This is also supported by the higher pH of RMGI and nano CaF_2 composite in Fig. 3, than the pH of CompositeNoF, at both 48 h and 72 h. These results are corroborated by the F-containing materials having lower lactic acid production and CFU (Fig. 5), and lower MTT absorbance (Fig. 6), than the commercial CompositeNoF. Therefore, the following two points should be noted: (1) While the release of Ca and PO_4 ions are beneficial in remineralization, the incorporation of CHX was needed in the ACP nanocomposite to maintained a safe pH of 6.5; (2) the additional F release of the nano CaF_2 + CHX composite was beneficial in further reducing the lactic acid production of bacteria.

Compared to the CompositeNoF, the biofilm acid production on nano ACP + CHX and nano CaF_2 + CHX composites was reduced by 10 fold. The MTT absorbance, related to the bacteria metabolism, was reduced by 10-20 fold. The flexural strength and elastic modulus of the nanocomposites with CHX were not significantly different from those of CompositeNoF after 28 d of immersion. According to the manufacturer, CompositeNoF (Renamel) is indicated for Class III, IV, and V restorations. This suggests that the new nanocomposites containing fine CHX particles may also be suitable for these applications. Further study is needed to improve and optimize the ACP and CaF_2 nanocomposites, and to systematically investigate their mechanical and physical properties as well as anti-caries capabilities.

5. Summary

This study developed novel nanocomposites containing ACP and CaF_2 nanoparticles and

CHX, and determined their effects on bacteria growth, biofilm formation, acid production and colony-forming units for the first time. Compared to commercial control composites, nano ACP composite had minimal antibacterial property, and nano CaF_2 composite had a moderate antimicrobial effect. In contrast, incorporating CHX into ACP and CaF_2 nanocomposites imparted potent antibacterial capabilities. The ACP and CaF_2 nanocomposites containing CHX maintained a *S. mutans* culture media pH of above 6.5, while that of commercial composites decreased to 4.2 which could cause tooth mineral dissolution. The nanocomposites with CHX reduced the biofilm acid production and metabolic activity by 10-20 times, compared to a commercial composite. Mechanical properties of the nanocomposites with CHX were similar to those of a commercial composite without fluoride nor CHX. These novel nanocomposites have the potential: (1) to release Ca and PO_4 ions to remineralize the existing lesions, and fluoride ions to form fluoroapatite to resist acid attacks; (2) to be used in moderate load-bearing restorations similar to commercial microfill composites; and (3) to inhibit biofilm formation, lactic acid production and dental caries. Further studies are needed to optimize the nanocomposite microstructure and investigate the antimicrobial and anti-caries capabilities.

Acknowledgments

We gratefully thank Dr. L. C. Chow and Dr. S. Takagi of the Paffenbarger Research Center of the American Dental Association Foundation (ADAF), and Dr. J. M. Antonucci of the National Institute of Standards and Technology (NIST) for discussions. This study was supported by NIH R01 grants DE17974 and DE14190 (HX), NIDCR Interagency Agreement to NIST ( ), the University of Maryland Dental School, NIST, and the West China College of Stomatology.

Disclaimer

Certain commercial materials and equipment are identified to specify experimental procedures. This does not imply recommendation by NIST.

References

[1] American Dental Association (ADA). The 1999 survey of dental services rendered. Chicago, IL: ADA Survey Center, 2002.

[2] Ferracane JL. Current trends in dental composites. Crit Rev Oral Biol Med 1995;6:302-318.

[3] Bayne SC, Thompson JY, Swift EJ, Stamatiades P, Wilkerson M. A characterization of first-generation flowable composites. J Am Dent Assoc 1998;129:567-577.

[4] Imazato S. Review: Antibacterial properties of resin composites and dentin bonding systems. Dent Mater 2003;19:449-457.

[5] Xu X, Ling L, Wang R, Burgess JO. Formation and characterization of a novel fluoride-releasing dental composite. Dent Mater 2006;22:1014-1023.

[6] Krämer N, García-Godoy F, Reinelt C, Frankenberger R. Clinical performance of posterior compomer restorations over 4 years. Am J Dent 2006;19:61-66.

[7] Garoushi S, Vallittu PK, Watts DC, Lassila LV. Effect of nanofiller tractions and temperature on polymerization shrinkage on glass fiber reinforced filling material. Dent Mater 2008;24:606-610.

[8] Drummond JL. Degradation, fatigue, and failure of resin dental composite materials. J Dent Res 2008;87:710-719.

[9] Lim BS, Ferracane JL, Sakaguchi RL, Condon JR. Reduction of polymerization

contraction stress for dental composites by two-step light-activation. Dent Mater 2002;18:436-444.

[10] Ruddell DE, Maloney MM, Thompson JY. Effect of novel filler particles on the mechanical and wear properties of dental composites. Dent Mater 2002;18:72-80.

[11] Drummond JL, Bapna MS. Static and cyclic loading of fiber-reinforced dental resin. Dent Mater 2003;19:226-231.

[12] Lu H, Stansbury JW, Bowman CN. Impact of curing protocol on conversion and shrinkage stress. J Dent Res 2005;84:822-826.

[13] Ferracane JL. Hygroscopic and hydrolytic effects in dental polymer networks. Dent Mater 2006;22:211-222.

[14] Watts DC, Issa M, Ibrahim A, Wakiaga J, Al-Samadani K, Al-Azraqi M *et al.* Edge strength of resin-composite margins. Dent Mater 2008;24:129-133.

[15] Rodrigues SA, Scherrer SS, Ferracane JL, Bona AD. Microstructural characterization and fracture behavior of a microhybrid and a nanofill composite. Dent Mater 2008;24:1281-1288.

[16] Mjör IA, Moorhead JE, Dahl JE. Reasons for replacement of restorations in permanent teeth in general dental practice. International Dent J 2000;50:361-366.

[17] Sarrett DC. Clinical challenges and the relevance of materials testing for posterior composite restorations. Dent Mater 2005;21:9-20.

[18] Sakaguchi RL. Review of the current status and challenges for dental posterior restorative composites: clinical, chemistry, and physical behavior considerations. Dent Mater 2005;21:3-6.

[19] Deligeorgi V, Mjor IA, Wilson NH. An overview of reasons for the placement and

replacement of restorations. Prim Dent Care 2001;8:5-11.

[20] Frost PM. An audit on the placement and replacement of restorations in a general dental practice. Prim Dent Care 2002;9:31-36.

[21] Jokstad A, Bayne S, Blunck U, Tyas M, Wilson N. Quality of dental restorations. FDI Commision Projects 2-95. International Dent J 2001;51:117-158.

[22] Loesche WJ. Role of Streptococcus mutans in human dental decay. Microbiological Reviews 1986;50:353-380.

[23] van Houte J. Role of micro-organisms in caries etiology. J Dent Res 1994;73:672-681.

[24] Featherstone JD. The science and practice of caries prevention. J Am Dent Assoc 2000;131:887-899.

[25] Featherstone JD. The continuum of dental caries - Evidence for a dynamic disease process. J Dent Res 2004;83:C39-C42.

[26] Deng DM, ten Cate JM. Demineralization of dentin by Streptococcus mutans biofilms grown in the constant depth film fermentor. Caries Res 2004;38:54-61.

[27] Totiam P, Gonzalez-Cabezas C, Fontana MR, Zero DT. A new *in vitro* model to study the relationship of gap size and secondary caries. Caries Res 2007;41:467-473.

[28] Svanberg M, Mjör IA, Ørstavik D. Mutans streptococci in plaque from margins of amalgam, composite, and glass-ionomer restorations. J Dent Res 1990;69;861-864.

[29] Imazato S, Torii M, Tsuchitani Y, McCabe JF, Russell RRB. Incorporation of bacterial inhibitor into resin composite. J Dent Res 1994;73;1437-1443.

[30] Sousa RP, Zanin IC, Lima JP, Vasconcelos SM, Melo MA, Beltrao HC *et al. In situ* effects of restorative materials on dental biofilm and enamel demineralization. J Dent 2009;37:44-51.

[31] Thome T, Mayer MPA, Imazato S, Geraldo-Martins VR, Marques MM. *In vitro* analysis of inhibitory effects of the antibacterial monomer MDPB-containing restorations on the progression of secondary root caries. J Dent 2009;37:705-711.

[32] Antonucci JM, Zeiger DN, Lin-Gibson S, Fowler BO, Lin NJ. Synthesis and characterization of antimicrobial dimethacrylates containing quaternary ammonium functionalities for dental and biomedical applications. Dent Mater (2011, in press).

[33] Patel MP, Cruchley AT, Coleman DC, Swai H, Braden M, Williams DM. A polymeric system for the intra-oral delivery of an anti-fungal agent. Biomaterials 2001;22:2319-2324.

[34] Leung D, Spratt DA, Pratten J, Gulabivala K, Mordan NJ, Young AM. Chlorhexidine-releasing methacrylate dental composite materials. Biomaterials 2005;26:7145-7153.

[35] Anusavice KJ, Zhang NZ, Shen C. Controlled release of chlorhexidine from UDMA-TEGDMA resin. J Dent Res 2006;85:950-954.

[36] Palmer G, Jones FH, Billington RW, Pearson GJ. Chlorhexidine release from an experimental glass ionomer cement. Biomaterials 2004;25:5423-5431.

[37] Takahashi Y, Imazato S, Kaneshiro A, Ebisu S, Frenchen JE, Tay FR. Antibacterial effects and physical properties of glass-ionomer cements containing chlorhexidine for the ART approach. Dent Mater 2006;22:647-652.

[38] Skrtic D, Antonucci JM, Eanes ED, Eichmiller FC, Schumacher GE. Physiological evaluation of bioactive polymeric composites based on hybrid amorphous calcium phosphates. J Biomed Mater Res B 2000;53:381-391.

[39] Dickens SH, Flaim GM, Takagi S. Mechanical properties and biochemical activity of remineralizing resin-based Ca-PO_4 cements. Dent Mater 2003;19:558-566.

[40] Langhorst SE, O'Donnell JNR, Skrtic D. *In vitro* remineralization of enamel by polymeric amorphous calcium phosphate composite: Quantitative microradiographic study. Dent Mater 2009;25:884-891.

[41] Xu HHK, Sun L, Weir MD, Antonucci JM, Takagi S, Chow LC. Nano dicalcium phosphate anhydrous-whisker composites with high strength and Ca and PO_4 release. J Dent Res 2006;85:722-727.

[42] Xu HHK, Weir MD, Sun L, Moreau JL, Takagi S, Chow LC *et al.* Strong nanocomposites with Ca, PO_4 and F release for caries inhibition. J Dent Res 2010;89:19-28.

[43] Xu HHK, Moreau JL, Sun L, Chow LC. Strength and fluoride release characteristics of a calcium fluoride based dental nanocomposite. Biomaterials 2008;29:4261-4267.

[44] Xu HHK, Moreau JL, Sun L, Chow LC. Novel CaF_2 nanocomposite with high strength and F ion release. J Dent Res 2010;89:739-745.

[45] Xu HHK, Moreau JL, Sun L, Chow LC. Nanocomposite containing amorphous calcium phosphate nanoparticles for caries inhibition. Dent Mater 2011 (in review).

[46] Chow LC, Sun L, Hockey B. Properties of nanostructured hydroxyapatite prepared by a spray drying technique. J Res NIST 2004;109:543-551.

[47] Sun L, Chow LC. Preparation and properties of nano-sized calcium fluoride for dental applications. Dent Mater 2008;24:111-116.

[48] Moreau JL, Sun L, Chow LC, Xu HHK. Mechanical and acid neutralizing properties and inhibition of bacterial growth of amorphous calcium phosphate dental nanocomposite. J Biomed Mater Res B (2011, accepted for publication).

[49] Lee Y, Lu H, Oguri M, Powers JM. Changes in gloss after simulated generalized wear of

composite resins. J Prosthet Dent 2005;94:370-376.

[50] Exterkate RA, Crielaard W, Ten Cate JM. Different response to amine fluoride by *Streptococcus mutans* and polymicrobial biofilms in a novel high-throughput active attachment model. Caries Res 2010;44:372-379.

[51] van Loveren C, Buijs JF, ten Cate JM. The effect of triclosan toothpaste on enamel demineralization in a bacterial demineralization model. J Antimicrob Chemo 2000 45:153-158.

[52] Mosmann T. Rapid colorimetric assay for cellular growth and survival: application to proliferation and cytotoxicity assays. J Immunol Methods 1983;65:55-63.

[53] Hiom SJ, Furr JR, Russell AD, Dickinson JR. Effects of chlorhexidine diacetate on *Candida albicans, C glabrata* and *Saccharomyces cerevisae*. J Appl Bacteriol 1996;72:335-340.

[54] Giuliana G, Pizzo G, Milici ME, Musotto GC, Giangreco R. *In vitro* antifungal properties of mouthrinses containing antimicrobial agents. J Periodontol 1997;68:729-733.

[55] Stoodley P, Wefel J, Gieseke A, deBeer D, von Ohle C. Biofilm plaque and hydrodynamic effects on mass transfer, fluoride delivery and caries. J Am Dent Assoc 2008;139:1182-1190.

[56] Dawes C. What is the critical pH and why does a tooth dissolve in acid? J Can Dent Assoc 2003;69:722-724.

[57] Burne RA. Oral *Streptococci* … Products of their environment. J Dent Res 1998;77:445-452.

[58] Deng DM, van Loveren C, ten Cate JM. Caries-preventive agents induce

remineralization of dentin in a biofilm model. Caries Res 2005;39-216-223.

Figure Captions

[1] SEM micrographs of the ground chlorhexidine (CHX) particles. (A) A pile of particles at a lower magnification. (B) Dispersed particles at a higher magnification. (C) CHX particle size distribution, based on the measurement via SEM of 100 random particles. (D) CHX release from the nano ACP composite and nano CaF_2 composite. Each value is the mean of three measurements with the error bar showing one standard deviation (mean ± sd; n = 3), with specimens immersed in a physiological-like solution at pH 7 from 1 d to 28 d.

[2] Mechanical properties of various restorative materials after 1 d and 28 immersion: (A) Flexural strength, and (B) elastic modulus. Each value is mean ± sd; n = 6. CompositeF is Heliomolar. CompositeNoF is Renamel. RMGI is Vitremer. NanoACP composite and nanoCaF_2 composite had no CHX. Nano ACP + CHX composite and nano CaF_2 + CHX composite contained 10% CHX particles by mass.

[3] The pH of the culture media with biofilm on the composite disk. Each value is mean ± sd; n = 6. During the first 24 h after inoculation, an initial biofilm was established on the composite disk. At 24 h, the disk was transferred to a new well with new media, and the pH measurement was started. The plot in (A) shows the pH from 24 h to 48 h. At 48 h, a new culture media was used (because the media was changed daily), and the pH is plotted in (B) from 48 h to 72 h. The initial pH was 7.2 for each new media.

[4] Live/dead staining photos: Initial biofilms (1 d) are shown for (A) CompositeF, (B) RMGI, (C) nano ACP composite, and (D) nano ACP + CHX composite. Mature biofilms

(3 d) are shown for the same materials in (E) to (H). Live bacteria were stained green, and dead bacteria were stained a red/orange color. At 1 d, bacteria were mostly alive in (A) to (C). (D) Nano ACP + CHX composite had dead bacteria. At 3 d, live bacteria formed mature and thick biofilms in (E) to (G). (H) Nano ACP + CHX composite had few bacteria on its surface. Photos for CompositeNoF and nano CaF_2 composite were not shown to save space, and they had qualitatively similar features to the other materials without CHX. Photos for nano CaF_2 + CHX composite was not shown, but it had similar features to nano ACP + CHX composite.

[5] Quantitative response of *S. mutans* biofilms on the composite disks: (A) Lactic acid production, and (B) bacteria colony-forming units (CFU) on the disks at 3 d. In each plot, dissimilar letters indicate values (mean ± sd; n = 6) that are different from each other ($p < 0.05$). Values with the same letters are not significantly different ($p > 0.1$).

[6] Results of the MTT metabolic assay for *S. mutans* on composite disks at: (A) 1 d, and (B) 3 d. A higher absorbance indicates a higher number of live bacteria on the composite disk that metabolized the MTT tetrazole. In each plot, values (mean ± sd; n = 6) with dissimilar letters are significantly different from each other ($p < 0.05$). Values with the same letters are not significantly different ($p > 0.1$).

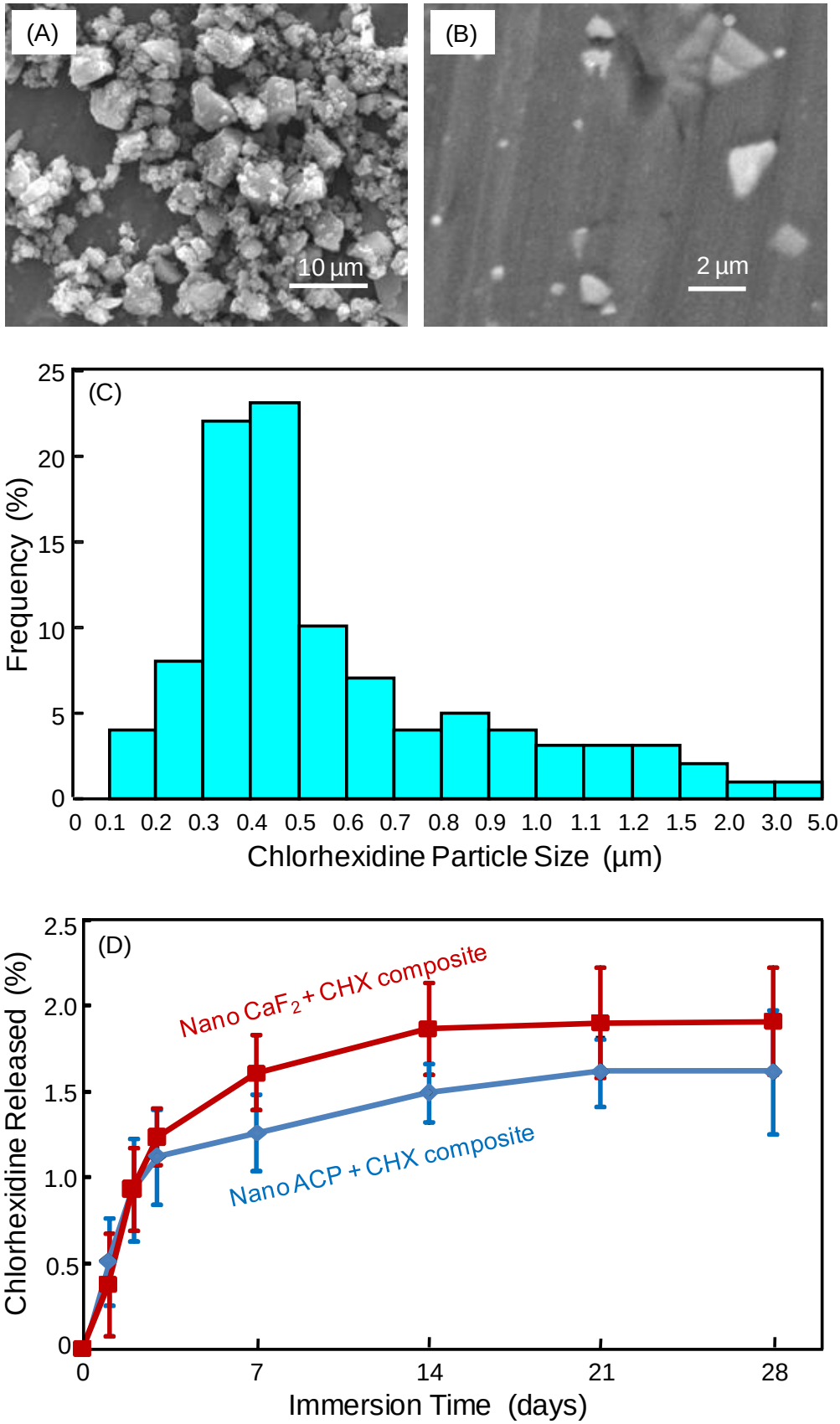
(A)
10 µm
(B)
2 µm
(C)
Frequency (%)
0
5
10
15
20
25
0 0.1 0.2 0.3 0.4 0.5 0.6 0.7 0.8 0.9 1.0 1.1 1.2 1.5 2.0 3.0 5.0
Chlorhexidine Particle Size (µm)
(D)
Chlorhexidine Released (%)
0
0.5
1.0
1.5
2.0
2.5
Nano CaF2 + CHX composite
Nano ACP + CHX composite
0
7
14
21
28
Immersion Time (days)

Fig.1

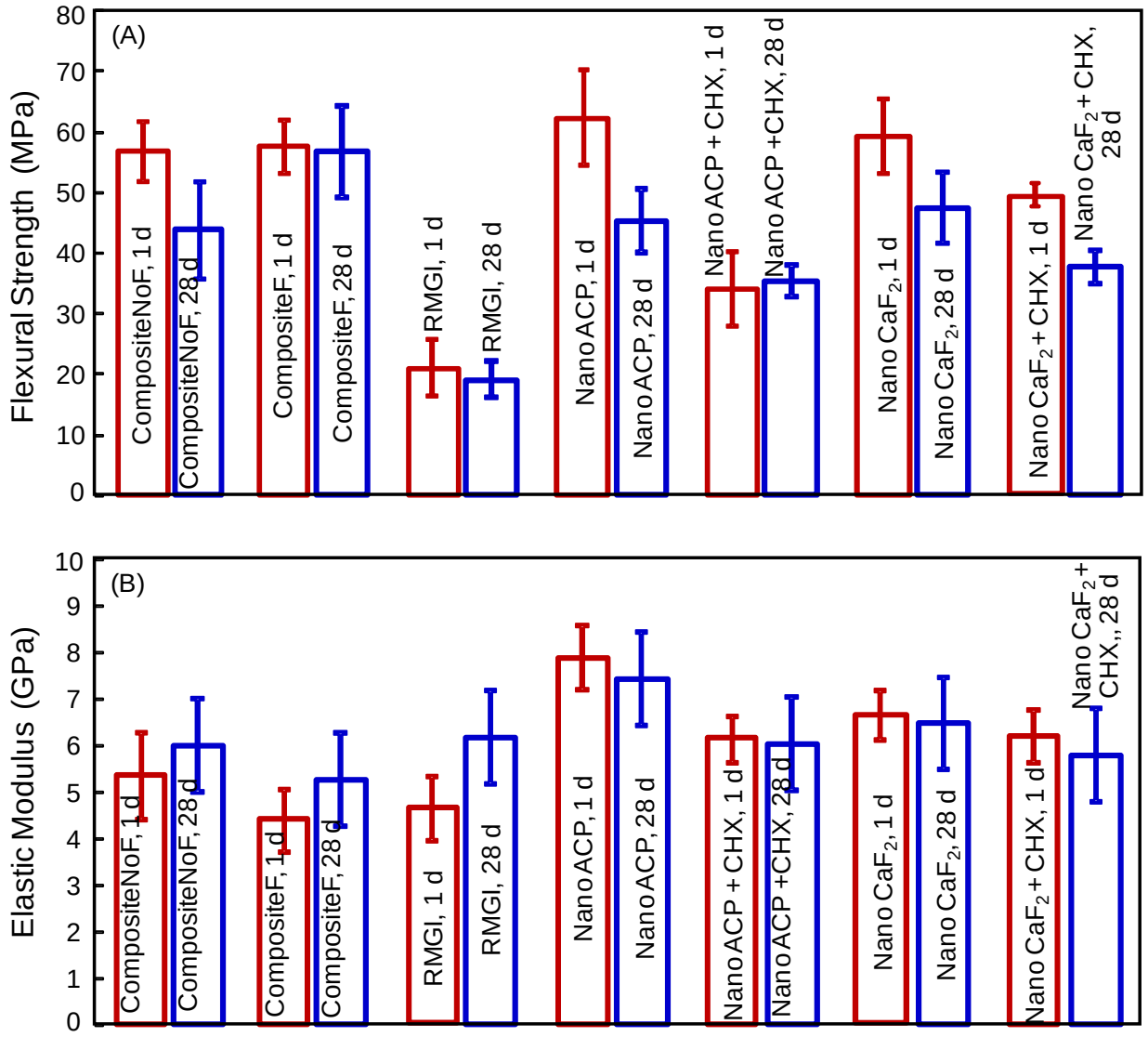
(A)
Flexural Strength (MPa)
0
10
20
30
40
50
60
70
80
CompositeNoF, 1 d
CompositeNoF, 28 d
CompositeF, 1 d
CompositeF, 28 d
RMGI, 1 d
RMGI, 28 d
Nano ACP, 1 d
Nano ACP, 28 d
Nano ACP + CHX, 1 d
Nano ACP +CHX, 28 d
Nano CaF2, 1 d
Nano CaF2, 28 d
Nano CaF2 + CHX, 1 d
Nano CaF2 + CHX, 28 d
(B)
Elastic Modulus (GPa)
0
1
2
3
4
5
6
7
8
9
10
CompositeNoF, 1 d
CompositeNoF, 28 d
CompositeF, 1 d
CompositeF, 28 d
RMGI, 1 d
RMGI, 28 d
Nano ACP, 1 d
Nano ACP, 28 d
Nano ACP + CHX, 1 d
Nano ACP +CHX, 28 d
Nano CaF2, 1 d
Nano CaF2, 28 d
Nano CaF2 + CHX, 1 d
Nano CaF2 + CHX,, 28 d

Fig. 2

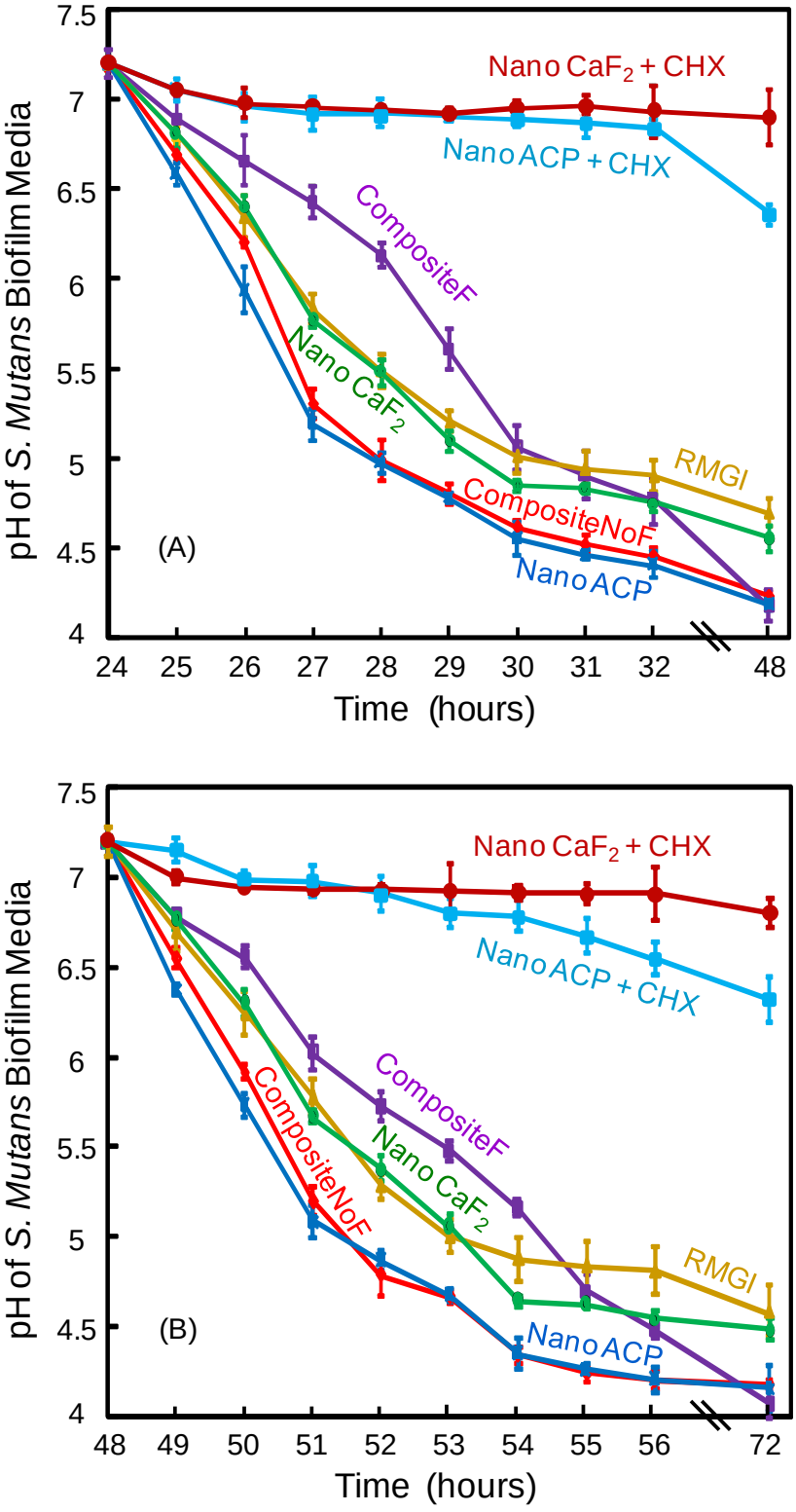
pH of S. Mutans Biofilm Media
Time (hours)
Nano CaF2 + CHX
Nano ACP + CHX
CompositeF
Nano CaF2
RMGI
CompositeNoF
Nano ACP
(A)
(B)

Figure 3

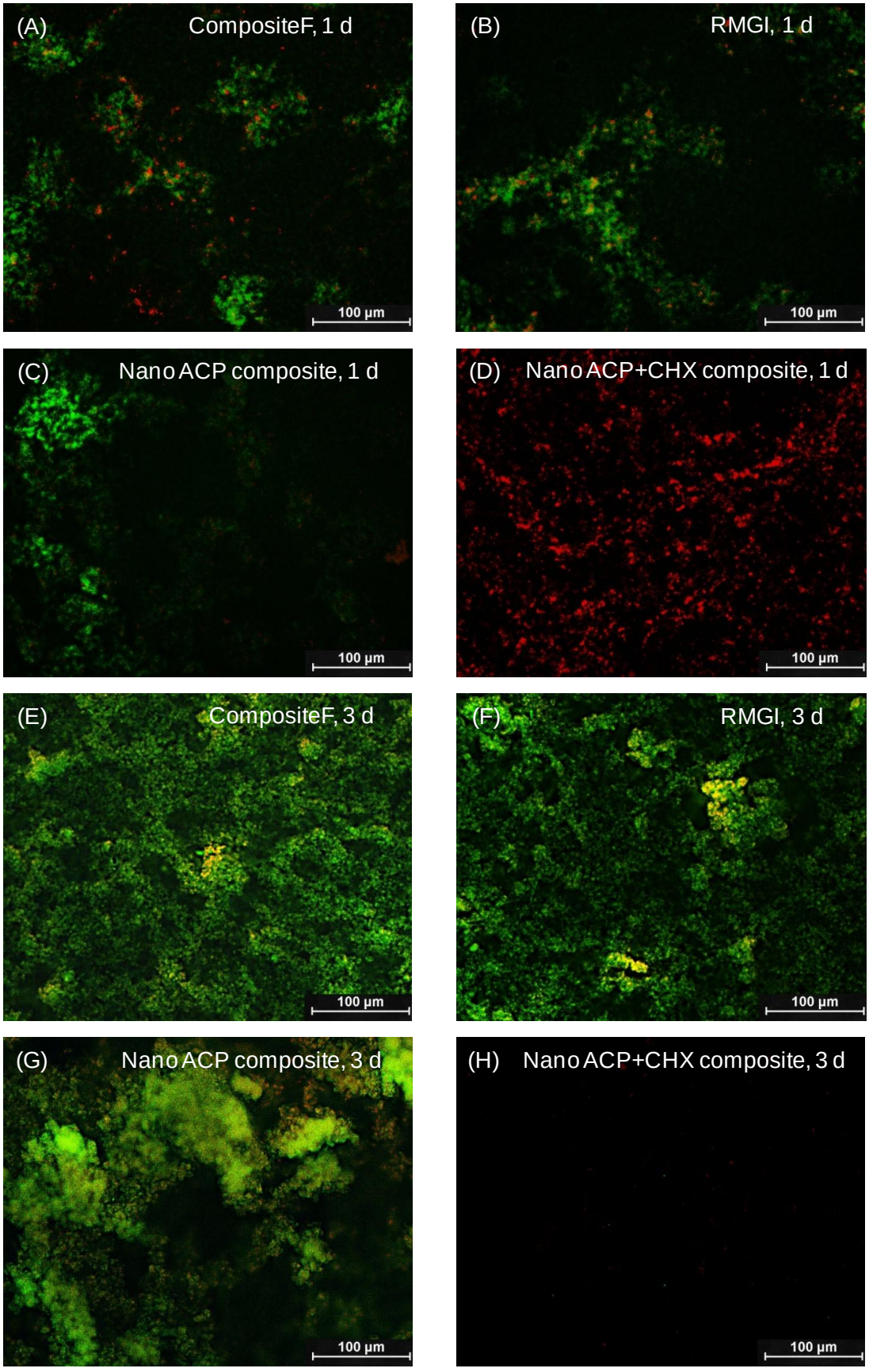
(A) CompositeF, 1 d
100 μm
(B) RMGI, 1 d
100 μm
(C) Nano ACP composite, 1 d
100 μm
(D) Nano ACP+CHX composite, 1 d
100 μm
(E) CompositeF, 3 d
100 μm
(F) RMGI, 3 d
100 μm
(G) Nano ACP composite, 3 d
100 μm
(H) Nano ACP+CHX composite, 3 d
100 μm

Fig 4

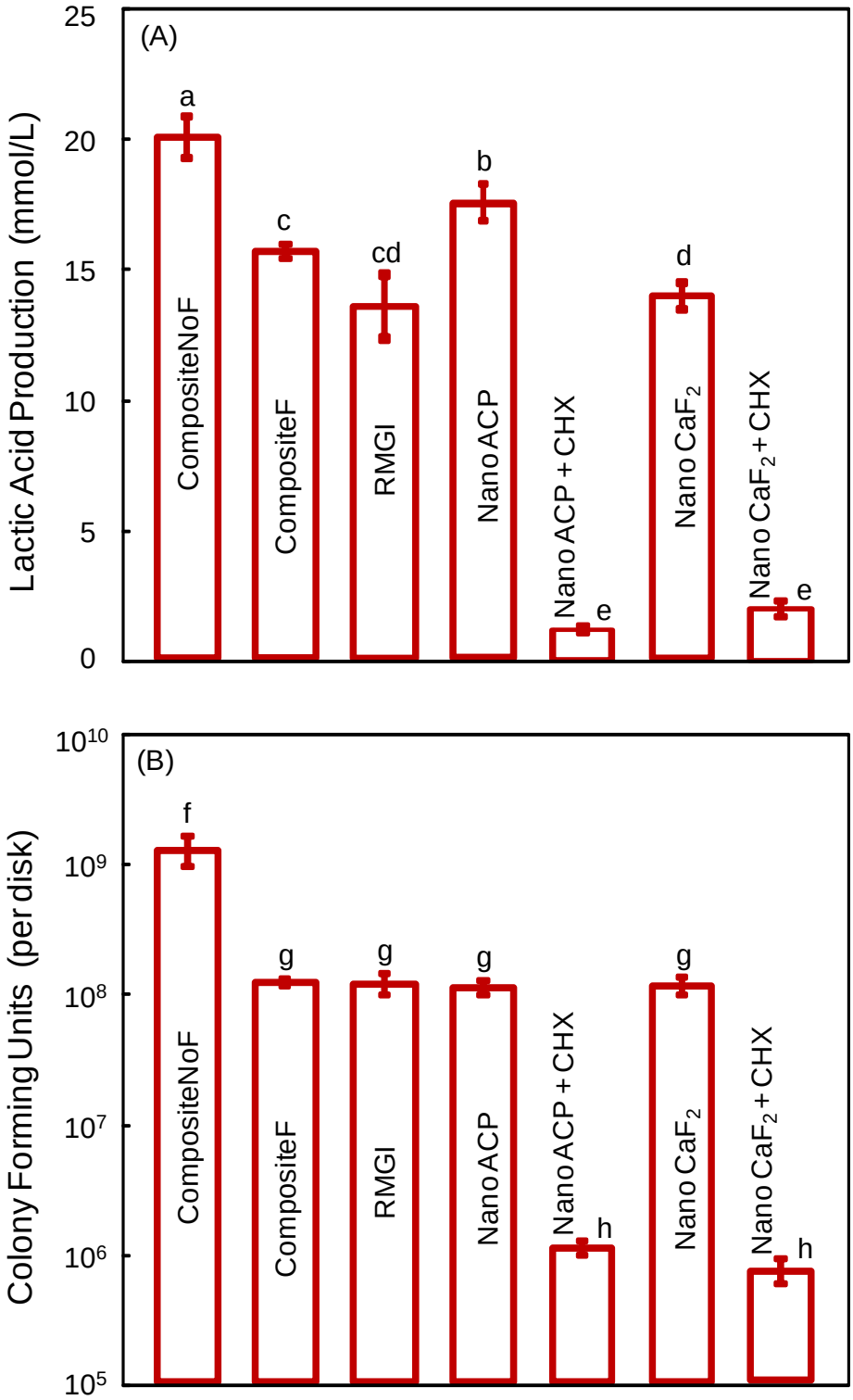
(A)
Lactic Acid Production (mmol/L)
25
20
15
10
5
0
a
c
cd
b
e
d
e
CompositeNoF
CompositeF
RMGI
Nano ACP
Nano ACP + CHX
Nano CaF_2
Nano CaF_2 + CHX
(B)
Colony Forming Units (per disk)
10^{10}
10^{9}
10^{8}
10^{7}
10^{6}
10^{5}
f
g
g
g
h
g
h
CompositeNoF
CompositeF
RMGI
Nano ACP
Nano ACP + CHX
Nano CaF_2
Nano CaF_2 + CHX

Fig. 5

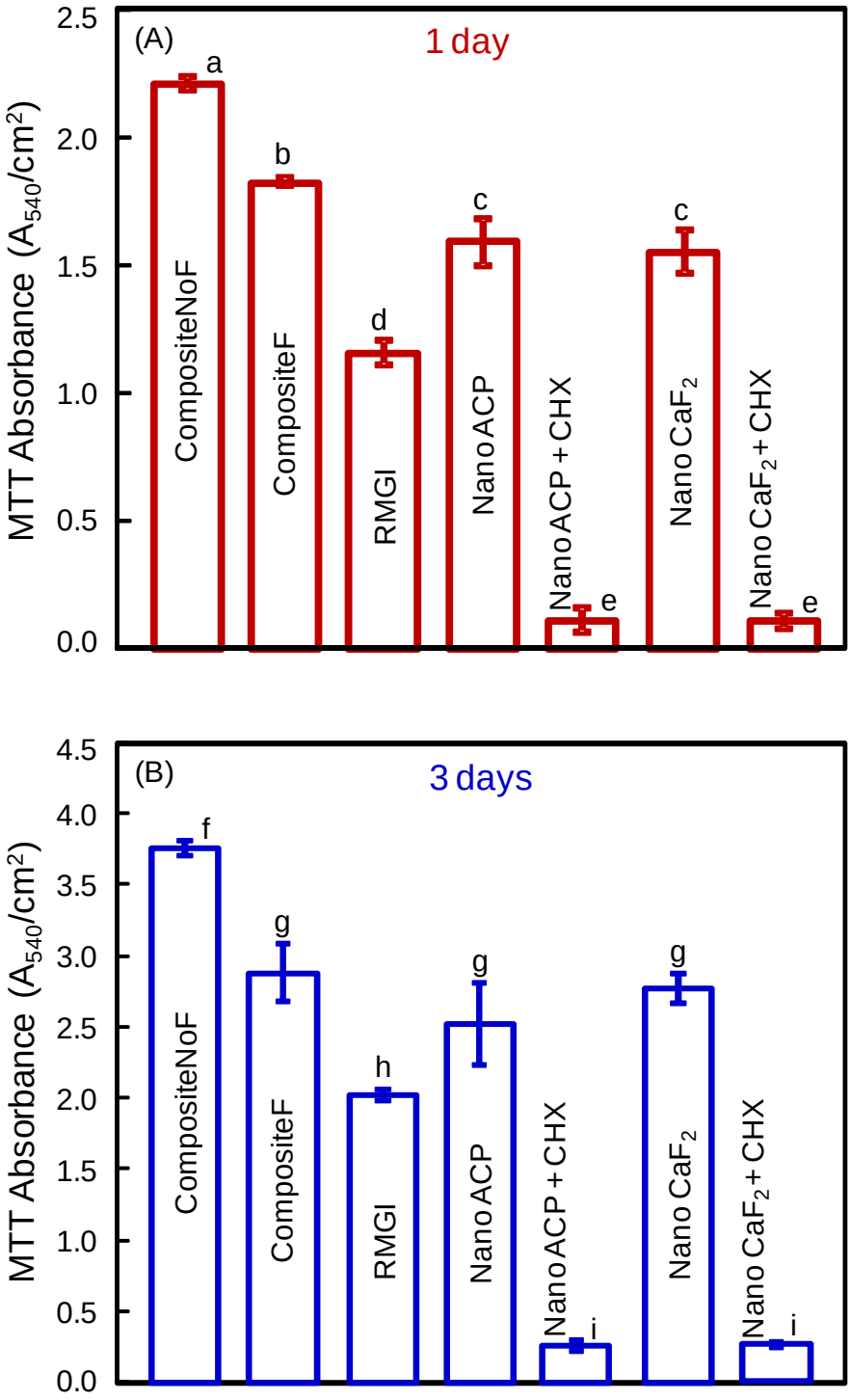
(A)
1 day
MTT Absorbance (A540/cm2)
2.5
2.0
1.5
1.0
0.5
0.0
a
b
c
d
c
e
e
CompositeNoF
CompositeF
RMGI
Nano ACP
Nano ACP + CHX
Nano CaF2
Nano CaF2 + CHX
(B)
3 days
MTT Absorbance (A540/cm2)
4.5
4.0
3.5
3.0
2.5
2.0
1.5
1.0
0.5
0.0
f
g
h
g
i
g
i
CompositeNoF
CompositeF
RMGI
Nano ACP
Nano ACP + CHX
Nano CaF2
Nano CaF2 + CHX

Fig. 6